Journal of
Nanoelectronics and Optoelectronics
Vol. 2, 1–6, 2007

Properties of Planar Electric Metamaterials for Novel Terahertz Applications

John F. O'Hara[1,*], Evgenya Smirnova[2], Hou-Tong Chen[1], Antoinette J. Taylor[1], Richard D. Averitt[1], Clark Highstrete[3], Mark Lee[3], and Willie J. Padilla[4]

[1] *MPA-CINT, Los Alamos National Laboratory, Los Alamos, NM 87545, USA*
[2] *ISR-6, Los Alamos National Laboratory, Los Alamos, NM 87545, USA*
[3] *Sandia National Laboratories, Albuquerque, NM 87185, USA*
[4] *Department of Physics, Boston College, Chestnut Hill, MA 02467, USA*

Planar electric metamaterials are experimentally studied in transmission and reflection utilizing terahertz time-domain spectroscopy. Electrically resonant behavior is observed and provides an estimate of the frequency-dependent transmissivity, reflectivity, and absorptivity of metamaterial composites. Numerical simulations are in good agreement with the measured results and provide additional information helpful in understanding their electromagnetic response. Our results and approach help define the boundaries of a metamaterials-based design paradigm and should prove beneficial in future terahertz applications, particularly with respect to novel filtering, modulation, and switching devices. In addition, this work clarifies some of the mechanisms that limit efficient metamaterials operation at higher-frequencies.

Keywords: Metamaterials, Terahertz, Optical Materials, Resonance, Microstructure Devices.

RESEARCH ARTICLE

Recently, research into a new class of artificial composites, called metamaterials,[1] has seen an enormous amount of growth. Metamaterials are artificial electromagnetic materials typically comprised of periodic arrays of sub-wavelength ($\sim \lambda/10$) metallic resonators within or on a dielectric or semiconducting substrate. Due to the small size of the resonators, these composites can be considered effective media,[2] and can be quantitatively described by bulk constitutive parameters $\mu(\omega)$, and $\epsilon(\omega)$, in accordance with the macroscopic form of Maxwell's equations.[3,4] Metamaterials exhibit myriad functional properties not found in natural materials[5–7] including, as examples, negative refractive index and cloaking.[6,8] Many of these phenomena were predicted decades ago[9] but have only been experimentally realized using metamaterials during the past several years. The functional electromagnetic response of metamaterials arises from the ability to tune the resonant electric and/or magnetic response through design of the sub-wavelength resonator elements.[10] Furthermore, these resonant phenomena can be adjusted to occur at nearly any sub-optical (at present) region of the electromagnetic spectrum. Metamaterials, therefore, complement natural materials in terms of functional device designs and performance.

The terahertz (THz) spectrum (0.1–4 THz, $\lambda = 75$ μm–3 mm) represents a particularly interesting region in which to study metamaterials. Notably, the THz regime is becoming increasingly important in terms of closing the technology gap between optical and mm-wave device performance. However, there is a vivid lack of suitable materials from which to form the basic elements crucial to THz technology implementation on a large scale, even though the possible applications are numerous.[11–14] Presently, high-power THz sources, efficient detectors, switches, modulators, filters, and other basic elements are not widely available. Metamaterials are optimistic candidates to correct this problem.[15–17] Additionally, THz also serves as an ideal stage from which to investigate the dynamic nature and limitations of higher-frequency metamaterial designs. Though metamaterials designed for operation beyond the optical region are in principle possible, present-day fabrication techniques and inherent material limitations prevent their efficient operation. The information gleaned from THz metamaterials studies will become particularly relevant as new fabrication techniques and nano-technology solutions continue to enable ever smaller resonator structures. THz metamaterials research should, therefore, prove to be a very fruitful endeavor for both near-future and long-term technology growth.

*Author to whom correspondence should be addressed.

In this paper we study the behavior of planar THz metamaterials. All of our designs are based on the Babinet equivalent[20, 21] of the recently introduced electric resonator structures.[18, 19] While the tuning of both the magnetic and electric metamaterial response is sometimes desirable, certain applications such as filtering, can also benefit from these new metamaterials that exhibit a purely electrical response. Unlike conventional split-ring resonators (SRRs), these electrical metamaterials are based on resonator structures that are symmetrically designed to eliminate or minimize the magnetic effects caused by circulating currents. For all of our designs, measurements show a clear band-pass filtering effect in transmission, and a band-stop filtering effect in reflection. In conjunction with simulation results, these measurements also permit us to estimate the resonant absorptivity of the metamaterials.

The metamaterial samples used in this work are illustrated in Figure 1. These structures have an outer dimension of 36 μm, a lattice parameter of 50 μm, line widths of 4 μm, and gaps of 2 μm. They were fabricated by depositing the metal patterns in a square, planar array on semi-insulating gallium arsenide (SI-GaAs) of 625 μm thickness. Conventional photolithographic methods were employed and the metallization consisted of 200 nm of gold following 10 nm of titanium for adhesion. The structures were fabricated in the "inverse" configuration where metallization was present everywhere on the substrate except for the patterned resonators. In Figure 1 metallization is indicated by the gold color, whereas bare GaAs regions are shown in gray.

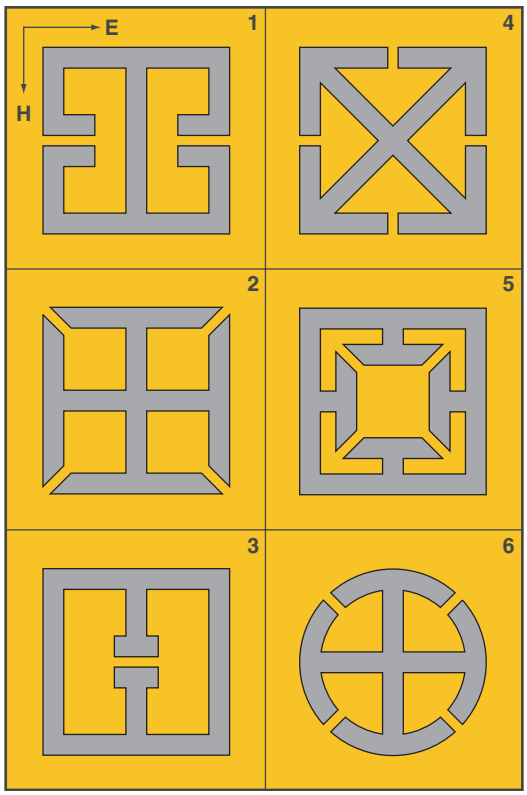

Fig. 1. Planar metamaterial unit cells with dimensions described in text. Gold color indicates metallized regions whereas gray color indicates bare SI-GaAs regions. The field polarization for normal incidence is shown near Sample #1. For oblique incidence (TM polarization) the magnetic field is unchanged but the electric field also has a component directed out of the plane of the page.

We used terahertz time-domain spectroscopy (THz-TDS)[22] to characterize the electromagnetic responses of the metamaterial structures. The THz-TDS system, shown in Figure 2 is a modified version of the system described elsewhere,[23] and is designed to allow the detector to be moved from a transmission to a reflection configuration. A fiber-optic system was used to deliver the dispersion compensated optical pulses to the detector thereby allowing detector translation without disturbing the laser alignment, the pulse timing, or the pulsewidth. Two Picarin[24] lenses were used to focus the THz beam to a frequency-independent spot approximately 3 mm ($1/e$) in diameter. The active areas of the samples were >1 cm square. Two additional confocal lenses were used to re-collimate and focus the transmitted or reflected beam back to the detector. The detector and its accompanying lenses were all attached to a single optical rail mounted on a large rotation stage to ensure their strict alignment regardless of detector positioning. The entire apparatus was enclosed in a large

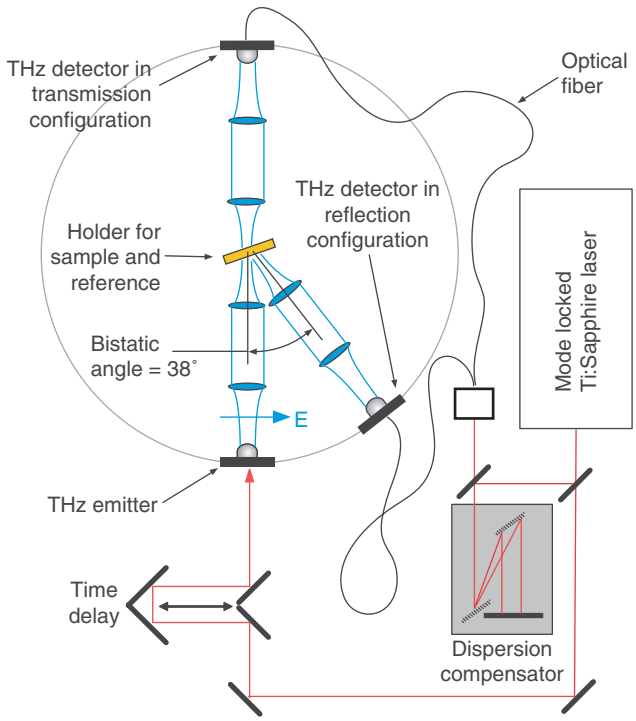

Fig. 2. THz time-domain spectroscopy setup. The THz beams, shown in blue, propagate with the polarization shown from the emitter to the samples mounted on a precisely aligned holder, shown in gold. An optical fiber permits the detector to be rotated around the sample to measure either transmission or reflection. Due to the close proximity of the focusing lenses to each other, reflection measurements were limited to 19° incidence.

box purged with dry air to mitigate the effects of water vapor.

Transmission measurements were performed on the samples and a bare SI-GaAs reference substrate of the same thickness. Measurements were taken at 19° incidence so that they could be directly compared to the reflection measurements, which were necessarily performed with the emitter and detector situated in a 38° bistatic configuration. Due to the orientation of the THz emitter, the polarization was transverse magnetic (TM). Figure 1 shows the orientation of this field with respect to the samples. Additional transmission measurements were performed at normal incidence to compare the effect of the incident field being in-plane versus out-of-plane with respect to the metamaterial samples. Since the THz system utilizes coherent detection, we record the time-varying electric field of the transmitted THz radiation following passage through the sample. Fourier transformation of the measured time-domain data then permits the extraction of the frequency dependent complex transmission coefficient, $\tilde{t}(\omega) = t(\omega)e^{i\phi(\omega)}$, from which the transmissivity, $T(\omega) = t^2(\omega)$, can be obtained.

Reflection measurements were performed similarly, but in this case a metallized SI-GaAs substrate served as a reference. The samples and reference were both mounted on a carefully aligned holder that ensured their reflection faces were co-planar to within approximately 10 μm. Fourier transformation was used in this case to extract the frequency dependent complex reflection coefficient, $\tilde{r}(\omega) = r(\omega)e^{i\phi\omega}$, from which the reflectivity, $R(\omega) = r^2(\omega)$, could be obtained. A unique feature of our measurement technique is that the reflected and transmitted waves are measured coherently. This permits the unambiguous determination of propagation constants (and hence material constitutive parameters) without interferometric techniques. While this phase-dependent information is not discussed here, it represents an important metamaterials research capability only recently extended beyond the microwave regime.

Figure 3 shows the frequency dependent transmissivities and reflectivities obtained from our measurements. All of the samples clearly exhibit a strongly resonant behavior between 0.5 and 1.0 THz in response to the electromagnetic field. Resonant transmissivities indicate that as much as 60% of the energy transmits through the sample while nearby surrounding frequencies are essentially fully blocked. Transmissivities extracted from the measured data $T(\omega)$ were normalized by a factor α before analysis and plotting in Figure 3. In this work $\alpha = 0.77$, and the reasons for this scaling are discussed in detail later. Compared to transmissivities, resonant reflectivities revealed a complementary behavior showing on-resonance reflection to be sharply lower than that of surrounding frequencies.

Since we measure both transmission and reflection we are also able to estimate the aborption of the metamaterial

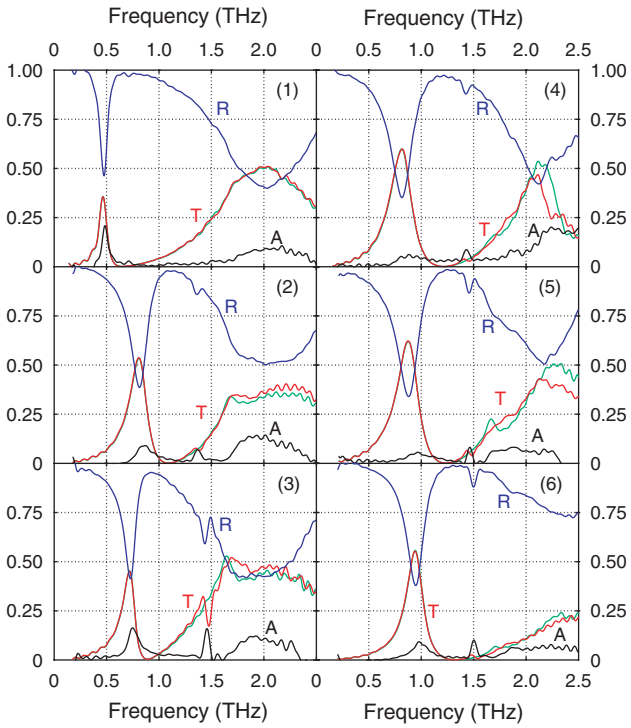

Fig. 3. Frequency dependent THz measured transmissivities (red for 19° incidence, green for normal incidence) and reflectivities (blue). Measured absorptivities, $A = 1 - (T + R)$, are shown in black.

composite. This information has been studied theoretically and shown to have important implications in metamaterial designs.[25] We initially measured the bare SI-GaAs substrate and found it to have very low absorption over the entire observed frequency range. Therefore, any absorption measured from the samples should be due only to the metamaterial composite. The absorptivity, $A(\omega)$, can be estimated by energy conservation, where $T(\omega) + R(\omega) + A(\omega) = 1$. It is clear from the data that in the spectral regions surrounding resonance the absorptivity of these samples must be very low since the sum of T and R is nearly unity. However, on resonance we observed absorptivities ranging from approximately 5–20%, depending on the sample. Additional "absorptive" behavior was observed above 1.5 THz. However simulation results indicate that these features are due to higher-order modes which scatter energy into non-specular directions as discussed below.

In order to assist our understanding of the data, we performed simulations of the electromagnetic response of the metamaterials using commercially available finite-element software;[26] the results are shown in Figure 4. Simulations were performed at normal incidence so some of the features differ slightly from the 19° data. These differences are discussed in context. Nevertheless, the simulations match the data very well with absorptivities ranging from 7–15%, indicating that our estimated absorptivities are accurate. We note this agreement applies only after scaling of the measured transmissivities by α.

RESEARCH ARTICLE

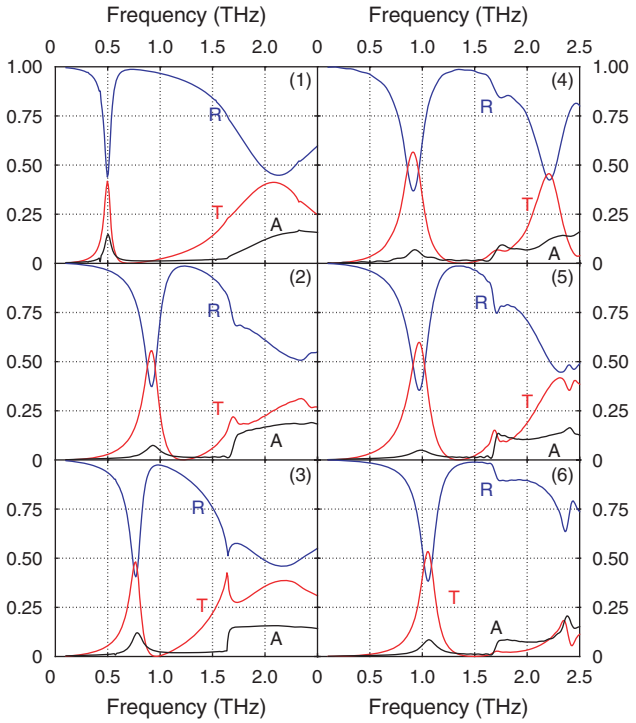

Fig. 4. Frequency dependent THz simulated transmissivities (red) and reflectivities (blue) at normal incidence. Simulated absorptivities, $A = 1 - (T + R)$, are shown in black.

Our justification for scaling the transmissivity data was, in part, based on these simulated results. First, it was found that in the absence of the correction the measured absorptivity became negative, implying gain within the metamaterial; the simulations did not suffer this physical impossibility. Second, it was found that only the transmissivity data needed scaling; the reflectivity simulation results matched the measured data with no scaling, as shown in Figures 3 and 4. The difference is due to the calculation of transmitted power from the experimental data versus the simulated transmission. In the case of the measurements a bare SI-GaAs substrate is used to collect a reference spectrum, which is divided out from the sample spectrum to obtain transmissivity. In principle this permits the cancelation of any of the effects from the underlying GaAs substrate, such as the Fresnel loss from the back face of the sample. However, in order for this operation to work properly the boundary between the metamaterial and the substrate must also be well-defined and distinct. This is a substantial approximation given the strong potentials and currents occurring on resonance around the perimeter of the thin metallic patterning. Instead of behaving like uniform plane-waves, these excitations more likely behave as highly sub-wavelength and isolated sources located at the surface of the GaAs substrate. Such sources are known to have complicated radiation patterns which preferentially radiate into the substrate.[27] Indeed similar mechanisms are observed in surface-plasmon mediated extraordinary transmission through sub-wavelength apertures.[28] Since the simulation software directly solves Maxwell's equations it can output absolute transmitted power without the problem of dividing out any reference.

In the case of the reflectivity, the software and data analysis are essentially equivalent. For the measured data, the fully metallized wafer serves as a nearly perfect reference. By reflecting ~100% of the incident power back to the detector it provides a known value to which the reflected power from the sample can be compared. This comparison does not depend at all on the background substrate. The simulation software performs the same procedure applying some known incident power to the sample and measuring the absolute reflected power. Since in reflection there are no complicated substrate effects the software and data analysis agree very well with no adjustments.

Finally, the transmissivity correction factor (α) was computed by forcing a match between simulated and measured transmission on resonance. The value α was an average value found to work well for all the samples. Since this correction was calculated on resonance, the fits at higher frequencies were not as close. This is expected however, since at these higher frequencies the metamaterial patterns no longer appear as highly sub-wavelength structures, so the behavior begins to approach that of the more familiar plane-wave excitation of a metal aperture. Given the excellent agreement in simulated and measured reflectivity, the correction factor obviously resulted in good agreement in absorptivity, particularly on resonance.

We now call attention to the spectral region in which agreements between measurement and simulation began to degrade. One prominent disagreement is found in the position of a small resonant feature, most obvious in Sample #3, occurring between 1.3–1.5 THz for the measured data, but occurring between 1.6–1.7 THz in simulation. In fact, this discrepancy only occurs because the measured data was collected at 19° incidence and the simulation was performed at normal incidence. The green curves in Figure 3 show the measured transmission data taken at normal incidence, in which case the position of this small resonance feature now agrees with simulation. Simulations further revealed that this feature is due to the onset of higher-order modes (HOMs). These HOMs are evanescent and do not propagate below their cutoff frequency, which was at normal incidence 1.64 THz, the exact location of the small resonant feature. However, above cutoff the HOMs can easily scatter energy into directions divergent from the fundamental. In the case of the simulation, this appears as an energy loss since the simulation plots show only power in the fundamental mode. Though our detector does not equally discriminate between modes, the presence of HOMs would have a similar effect as in simulation. In this case, the HOMs would simply scatter energy into undetectable directions, which would thus appear to be "absorptive" effects.

Obviously it is desirable in certain applications, such as filtering and modulation, to design metamaterials with very

highly resonant behavior. Therefore, these results have important implications in the design of metamaterial resonator structures. Our metamaterials exhibit a Lorentzian type resonant response which can be interpreted with the aid of the RLC circuit model.[29] The absorptivity in the metamaterial is the analogue to the RLC circuit resistance (R) and, based on the results in this work, it is clear that it plays an important role in the resonant interaction with the electromagnetic radiation. As the effect of R is eliminated the model tends toward a loss-free LC circuit, which has an infinite Q. Hence it's expected that sample absorptivities would have a close relationship to resonator Q's. The measured data does not reveal a clear relationship between absorptivity and resonator Q, though we note that simulations seem to indicate a possible correlation between higher absorption and sharper resonances. Sample #1, for example, has both the highest absorption and the sharpest resonance. Since the resonator Q is also determined by the resonator capacitance and inductance, these correlations are only speculative.

Our results have important implications for the design of metamaterials at higher frequencies. Since simulations were performed with a lossless GaAs substrate, and indeed our measured substrate was nearly lossless, we can conclude that the observed absorptivities are due to conduction losses within the metal patterning. This was further supported by other simulations in which the gold metallization was replaced by perfect electric conductors; a complete disappearance of the resonant absorption dip was observed. As metamaterial work is pushed to ever higher frequencies, metal losses become even more significant and it is desirable to predict what resonator structures will be least affected by this change. We point out near-infrared metamaterial demonstrations using planar split-ring resonators.[30] While resonant behavior is still observed, resonator Q's are degraded due to the inability to avoid damping effects within the metals and dielectrics forming the individual resonator structures.[31]

We next highlight some potential uses of the electric planar metamaterials presented here. The transmitted intensity shown in Figure 3 is essentially "complementary" compared to what was demonstrated for the electric resonator structures (i.e., band-pass character vs. band-stop) presented in the references.[19] Further structures detailed in Figure 1 have a relatively high volume fraction of metal. Thus they may serve as future grids or electrodes for biasing electronic components where a transparency window is desired. Existing "transparent" electrodes are constructed by simply fabricating the metallization to be extremely thin $\sim$10 nm. In cases where high current densities are needed, and/or simultaneous narrow-band filtering is required, the designs presented here offer obvious advantages. Further, dynamical or electrically controlled[16, 17] transparency within the THz regime is particularly attractive for potential applications, such as THz imaging. For example, by patterning semi-conductors within the capacitive gaps of the electric structures, or by forming diode structures utilizing these structures as gates, switching can be accomplished using either optical excitation of excess carriers to change the conductivity of the material in the capacitive gap, or using electrical carrier injection to change the conductivity of the switchable gap material. The range of properties accessible utilizing metamaterials provides significantly more flexibility than materials scientists and engineers are accustom to. Metamaterials present a new paradigm, using simple intuitive methods to design material structures that have a tailored electromagnetic response, leading to specifications that naturally and directly make use of this broad range of properties.

In conclusion, we have studied the behavior of a novel class of planar THz metamaterials through experimental THz time-domain transmission and reflection measurements. These materials exhibit strong resonances and distinct band-stop or band-pass filtering behavior in reflection and transmission, respectively. Through these measurements, we are able to estimate the absorptivity of the metamaterials, which ranges from 5–20% depending on the resonator design. In addition, we have found the origin of the resonant absorptivity to be Ohmic losses within the metallic patterning of the composites. Simulations are shown to greatly aid in the analysis of these materials and verify our measured results. Finally, our results provide demonstrations of the great flexibility in the metamaterial design approach.

They also illustrate some of intuitive design limitations for future THz and higher-frequency materials and devices. The continued research of the fundamental properties of metamaterials will have a great impact on many future novel metamaterial-based devices. This work was performed, in part, at the Center for Integrated Nanotechnologies, a U. S. Department of Energy, Office of Basic Energy Sciences, Nanoscale Science Research Center operated jointly by Los Alamos and Sandia National Laboratories. Los Alamos National Laboratory, an affirmative action/equal opportunity employer, is operated by Los Alamos National Security, LLC, for the National Nuclear Security Administration of the U. S. Department of Energy under contract DE-AC52-06NA25396.

RESEARCH ARTICLE

References and Notes

1. D. R. Smith, W. J. Padilla, D. C. Vier, S. C. Nemat-Nasser, and S. Schultz, *Phys. Rev. Lett.* 84, 4184 **(2000)**.
2. T. Koschny, M. Kafesaki, E. N. Economou, and C. M. Soukoulis, *Phys. Rev. Lett.* 93, 107402 **(2004).**
3. Th. Koschny, P. Markoš, E. N. Economou, D. R. Smith, D. C. Vier, and C. M. Soukoulis, *Phys. Rev. B* 71, 245105 **(2005)**.
4. For a review of the conditions of effective media applicable to metamterials see Ref. [3] and the references therin.
5. J. B. Pendry, *Phys. Rev. Lett.* 85, 3966 **(2000)**.
6. R. A. Shelby, D. R. Smith, and S. Schultz, *Science* 292, 77 **(2001)**.
7. D. Schurig and D. R. Smith, *Phys. Rev. E* 70, 065601(R) **(2004)**.
8. D. Schurig, J. J. Mock, B. J. Justice, S. A. Cummer, J. B. Pendry, A. F. Starr, and D. R. Smith, *Science* 314, 977 **(2006)**.

9. V. G. Veselago, *Sov. Phys. USPEKHI* 10, 509 **(1968)**.
10. J. B. Pendry, A. J. Holden, D. J. Robbins, and W. J. Stewart, *IEEE T. Microw. Theory* 47, 2075 **(1999)**.
11. J. E. Davis, *Infrared Phys.* 20, 287 **(1980)**.
12. D. A. Weitz, W. J. Skocpol, and M. Tinkham, *Opt. Lett.* 3, 13 **(1978)**.
13. F. Baumann, W. A. Bailey Jr., A. Naweed, W. D. Goodhue, and A. J. Gatesman, *Opt. Lett.* 28, 938 **(2003)**.
14. R. D. Rawcliffe and C. M. Randall, *Appl. Opt.* 6, 1353 **(1967)**.
15. T. J. Yen, W. J. Padilla, N. Fang, D. C. Vier, D. R. Smith, J. B. Pendry, D. N. Basov, and X. Zhang, *Science* 303, 1494 **(2004)**.
16. W. J. Padilla, A. J. Taylor, C. Highstrete, Mark Lee, and R. D. Averitt, *Phys. Rev. Lett.* 96, 107401 **(2006)**.
17. H.-T. Chen, W. J. Padilla, J. M. O. Zide, A. C. Gossard, A. J. Taylor, and R. D. Averitt, *Nature* **(2006)** (in press).
18. W. J. Padilla, M. T. Aronsson, C. Highstrete, Mark Lee, A. J. Taylor, and R. D. Averitt, Novel Electrically Resonant Terahertz Metamaterials, Los Alamos Pre-print server, http://xxx.lanl.gov/abs/cond-mat/0605002.
19. D. Schurig, J. J. Mock, and D. R. Smith, *Appl. Phys. Lett.* 88, 041109 **(2006)**.
20. Hou-Tong Chen, John F. O'Hara, Antoinette J. Taylor, Richard D. Averitt, C. Highstrete, Mark Lee, and Willie J. Padilla, unpublished.
21. F. Falcone, T. Lopetegi, M. A. G. Laso, J. D. Baena, J. Bonache, M. Beruete, R. Marqués, F. Martín, and M. Sorolla, *Phys. Rev. Lett.* 93, 197401 **(2004)**.
22. D. Grischkowsky, S. Keiding, M.Van Exter, and Ch. Fattinger, *J. Opt. Soc. Am. B* 7, 2006 **(1990)**.
23. John F. O'Hara, J. M. O. Zide, A. C. Gossard, A. J. Taylor, and R. D. Averitt, *Appl. Phys. Lett.* 88, 251119 **(2006)**.
24. Microtech Instruments Inc. Eugenee, OR 97401, USA, www.mtinstruments.com
25. S. O'Brien and J. B. Pendry, *J. Phys. Condens. Matter* 14, 6383 **(2002)**.
26. CST Microwave Studio®, © 2005 CST—Computer Simulation Technology, Wellesley Hills, MA, USA. www.cst.com.
27. David. B. Rutledge and Michael S. Muha, *IEEE T. Antenn. Propag.* AP-30, 535 **(1982)**.
28. Abul K. Azad and Weili Zhang, *Opt. Lett.* 30, 2945 **(2005)**.
29. Christophe Caloz and Tatsuo Itoh, Electromagnetic Metamaterials, Transmission Line Theory and Microwave Applications, John Wiley & Sons, Inc., Hoboken, NJ **(2006)**.
30. S. Linden, C. Enkrich, M. Wegener, J. Zhou, T. Koschny, and C. M. Soukoulis, *Science* 306, 1351 **(2004)**.
31. W. J. Padilla and D. R. Smith, *J. Opt. Soc. Am. B* 23, 404 **(2006)**.

Received: 22 November 2006. Revised/Accepted: 2 February 2007.